1-1-2008

Characterization and modeling of conjugated polymer sensors

Yang Fang
Michigan State University

Xiaobo Tan
Michigan State University

Andrew Temme
Michigan State University

Gursel Alici
University of Wollongong, gursel@uow.edu.au

Characterization and Modeling of Conjugated Polymer Sensors

Yang Fang [a], Xiaobo Tan [a], Andrew Temme [a], and Gürsel Alici [b]

[a]Smart Microsystems Laboratory, Department of Electrical & Computer Engineering,
Michigan State University, East Lansing, MI 48824, USA
[b]School of Mechanical, Materials, and Mechatronics Engineering,
University of Wollongong, 2522 NSW, Australia

ABSTRACT

In this paper the behavior of conjugated polymers as mechanical sensors is experimentally characterized and modeled. A trilayer conjugated polymer sensor is considered, where two polypyrrole (PPy) layers sandwich an amorphous polyvinylidene fluoride (PVDF) layer, with the latter serving as an electrolyte tank. A theory for the sensing mechanism is proposed by postulating that, through its influence on the pore structure, mechanical deformation correlates directly to the concentration of ions at the PPy/PVDF interface. This provides a key boundary condition for the partial differential equation (PDE) governing the ion diffusion and migration dynamics. By ignoring the migration term in the PDE, an analytical model is obtained in the form of a transfer function that relates the open-circuit sensing voltage to the mechanical input. The model is validated in experiments using dynamic mechanical stimuli up to 50 Hz.

Keywords: Conjugated polymer, polypyrrole (PPy), mechanical sensor, dynamic sensing model

1. INTRODUCTION

Flexible polymer sensors have broad applications because of their compact size, compliance, and light weight. Piezoelectric polymer sensors, in particular, polyvinylidene fluoride (PVDF), are already available commercially. The ionic electroactive polymers (ionic EAPs), which mainly include polyelectrolyte gels, ionic polymer-metal composites (IPMCs) and conjugated polymers, have shown promising applications in biomedical devices and micro robotics recently. The sensing properties of IPMCs and polyelectrolyte gels have been investigated and described as ion redistribution induced by the mechanical deformation.[1–4] Some researchers have also studied conjugated polymers' electrical response to mechanical deformation. Takashima *et al.* observed a mechanically induced electrochemical current in a free-standing film of polyaniline (PANI).[5] Madden observed the same effect in polypyrrole (PPy) and obtained the experimental value of strain-to-charge ratio.[6]

Research on modeling of conjugate polymers as electromechanical sensors has been relatively limited, comparing with the extensive work on modeling of conjugate polymer actuators.[6–10] Wu *et al.*[11] investigated the sensing behavior of a trilayer PPy beam by considering the perturbation of the Donnan equilibrium of the ion distribution by mechanical stimuli as the primary sensing mechanism. A similar viewpoint was also presented by Takashima and coworkers.[12] For better understanding of the sensing mechanisms, however, quantitative modeling of the sensing dynamics is desired.

In this paper, dynamic sensing behavior of conjugated polymers is experimentally characterized and mathematically modeled. A trilayer conjugated polymer sensor is considered, where two polypyrrole (PPy) layers sandwich an amorphous polyvinylidene fluoride (PVDF) layer, with the latter serving as an electrolyte tank. The model derivation starts with a partial differential equation (PDE) that governs the ion redistribution dynamics subject to diffusion and migration (due to electrostatic interactions). Two boundary conditions are postulated: 1) the ion concentration at the PPy/PVDF interface is proportional to the applied mechanical strain, as the latter directly influences the pore sizes of the PPy layer; and 2) there is no diffusion flux at the interface between the PPy layer and the air. This PDE can be solved numerically. However, for real-time sensing applications, it is desirable to have an analytical model. For this purpose, we ignore the migration term

Further author information: (Send correspondence to Xiaobo Tan.)
Yang Fang: E-mail: fangyang@msu.edu Telephone: 1-517-432-0437
Xiaobo Tan: E-mail: xbtan@msu.edu, Telephone: 1-517-432-5671
Andrew Temme: E-mail: temmeand@msu.edu
Gürsel Alici: E-mail: gursel@uow.edu.au

Electroactive Polymer Actuators and Devices (EAPAD) 2008, edited by Yoseph Bar-Cohen
Proc. of SPIE Vol. 6927, 692709, (2008) · 0277-786X/08/$18 · doi: 10.1117/12.776538

of the PDE, which makes the equation linear. The latter can be solved analytically in the Laplace domain, which leads to a transfer function that relates the open-circuit sensing voltage to the applied mechanical deformation. The obtained solution shows good approximation to the solution of the original PDE when the ion concentration is relatively low.

Experiments have been conducted to validate the proposed model. Sinusoidal displacements of 0.4 Hz to 50 Hz are applied through a custom-built apparatus. Experimental measurement of the open-circuit voltage matches the model prediction reasonably well. This work provides the first step towards fundamental understanding of mechanical sensing mechanisms of conjugated polymers.

The remainder of the paper is organized as follows. The full sensing model of the trilayer conjugated polymer beam and the approximated analytical model are described in Section 2. Experiments and discussions are presented in Section 3. Finally concluding remarks are provided in Section 4.

2. SENSING MODEL

2.1. Trilayer PPy structure

The trilayer PPy structure is shown in Fig. 1. In the middle is an amorphous, porous polyvinylidene fluoride (PVDF) layer that serves both as a backing material and storage for the electrolyte. PPy layers are on both sides of the PVDF layer. They were pre-doped with anions during synthesis, which was accomplished under oxidation. The electrolyte used is tetrabutylammonium hexafluorophosphate ($TBA^+PF_6^-$). Due to the constraint of PPy pore sizes, only anions (PF_6^-) can move in and out of the PPy layers.

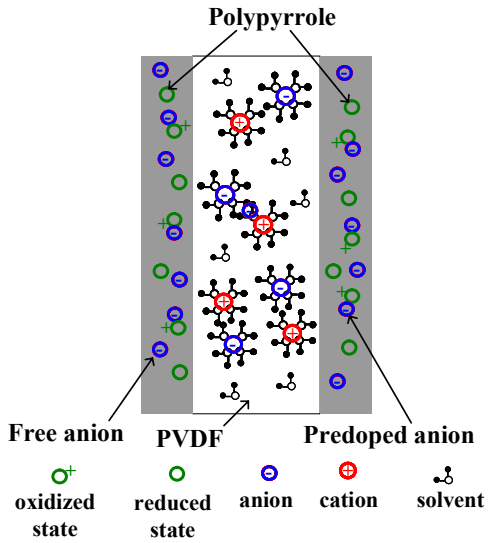

Figure 1. Illustration of the trilayer structure.

2.2. Full model

The Nernst-Planck equation is used widely to describe the flux of ions under the influence of both an ionic concentration gradient and an electric field:[13]

$$\mathbf{J} = -d(\nabla C + \frac{CF}{RT}\nabla\phi), \tag{1}$$

where d is the ionic diffusion coefficient, R is the gas constant, T is the absolute temperature, C is the mobile anion concentration, F is the Faraday constant, and ϕ is the electric potential. Besides, the continuity equation holds:

$$\nabla \cdot \mathbf{J} = -\frac{\partial C}{\partial t}. \tag{2}$$

One can relate ϕ to the ionic concentrations through the Gauss's law:

$$\mathbf{E} = \frac{D}{\kappa_e} = -\nabla\phi \tag{3}$$

$$\nabla \cdot \mathbf{D} = -FC, \tag{4}$$

where **D** denotes the electric displacement, **E** denotes the electric field, and κ_e is the dielectric permittivity of PPy. Since the thickness of the PPy layer is much smaller than its length or width, one can assume that, inside the polymer, **J**, **D**, **E**, and other changes are all restricted to the thickness direction (denoted as x direction). This enables one to drop the boldface notation for these variables; in particular, D and E will be used to represent the electric displacement and the electric field (along the x direction). From (2), we can derive

$$\frac{\partial C}{\partial t} = d\left(\frac{\partial^2 C}{\partial x^2} + \frac{F}{RT}\frac{\partial C}{\partial x}\frac{\partial \phi}{\partial x} + \frac{FC}{RT}\frac{\partial^2 \phi}{\partial x^2}\right). \tag{5}$$

The following can be derived based on (3) and (4):

$$\frac{\partial \phi}{\partial x} = \frac{F}{\kappa_e}\int_0^x C(\xi,t)d\xi + \frac{\partial \phi}{\partial x}(0,t), \tag{6}$$

$$\frac{\partial^2 \phi}{\partial x^2} = \frac{F}{\kappa_e}C(x,t). \tag{7}$$

In mechanical sensing, one can assume that $C(x,t)$ fluctuates about some equilibrium concentration C_0:

$$C(x,t) = C_0 + C_1(x,t), \tag{8}$$

with $C_0 \gg C_1(x,t)$. Further assume that the electrolyte has high ionic conductivity, which implies $\frac{\partial \phi}{\partial x}(0,t) = 0$ in (6). Therefore, (6) can be approximated by

$$\frac{\partial \phi}{\partial x} \approx \frac{FC_0}{\kappa_e}x. \tag{9}$$

Combining (5), (7), (8) and (9), and ignoring the C_1^2 term, one obtains

$$\frac{\partial C_1}{\partial t} = d\left(\frac{\partial^2 C_1}{\partial x^2} + \frac{F^2}{RT\kappa_e}\frac{\partial C_1}{\partial x}C_0 x + \frac{F^2}{RT\kappa_e}(C_0^2 + 2C_0C_1)\right). \tag{10}$$

Two boundary conditions are imposed on (10):

$$C_1(0,t) = KC_0\varepsilon_0(t), \tag{11}$$

$$\frac{\partial C_1}{\partial x}|_{x=h} = 0, \tag{12}$$

where $\varepsilon_0(t)$ represents the strain at the PPy/PVDF interface. Note that $x = 0$ denotes the PPy/PVDF boundary while $x = h$ denotes the PPy/air interface. The first boundary condition implies that the concentration perturbation at $x = 0$ has a linear correlation with the applied deformation. The second one means that there is no diffusion flux on the other side of the PPy layer.

Eq. (10) is difficult to solve analytically. In this paper, we have numerically solved for $C_1(x,t)$. The solution C_1 can then be integrated to obtain $D(x,t)$ using (4). Under the assumption that the electrolyte has very good ionic conductivity, one gets $D(0,t) = 0$ and thus $D(x,t)$ is expressed as

$$D(x,t) = -F\int_0^x C(\xi,t)d\xi, \tag{13}$$

where $C(\xi,t) = C_0 + C_1(\xi,t)$. Similarly one can integrate (3) and substitute (13) to get the voltage across the polymer as follows

$$\phi(x,t) - \phi(0,t) = \frac{F}{\kappa_e}\int_0^x \int_0^\delta C(\xi,t)d\xi d\delta. \tag{14}$$

Note that $\Delta V_1(t) = \phi(x,t) - \phi(0,t)$ represents the open-circuit sensing voltage induced on one PPy layer. One can obtain the sensing voltage $\Delta V_2(t)$ across the other PPy layer by following symmetric treatment. Finally, the total sensing signal is computed as

$$V(t) = \Delta V_1(t) - \Delta V_2(t). \tag{15}$$

2.3. Simplified model

It is desirable to obtain an analytical model for conjugated polymer sensors. Such a model can facilitate fundamental understanding of the sensing mechanisms and be instrumental in sensor design and real-time sensing applications. In this paper we obtain an analytical model from (10) by further ignoring the terms involving C_0. Equivalently, this is to ignore the effect of electric field-induced ion migration. The approximation is valid when the nominal anion concentration C_0 is low. The approximated PDE contains only the diffusion term:

$$\frac{\partial C_1}{\partial t} = d\frac{\partial^2 C_1}{\partial x^2}. \tag{16}$$

To solve this PDE, (16) is firstly converted into the Laplace domain

$$\frac{\partial^2 C_1(x,s)}{\partial x^2} = \frac{sC_1(x,s)}{d}. \tag{17}$$

Eq. (17) has a generic solution

$$C_1(x,s) = a_1(s)e^{-\sqrt{s/d}\,x} + a_2(s)e^{\sqrt{s/d}\,x}. \tag{18}$$

Letting $x = 0$ in (18) and using (11), one gets

$$a_1(s) + a_2(s) = KC_0\varepsilon_0(t). \tag{19}$$

From (18),

$$\frac{\partial C_1(x,s)}{\partial x} = -\sqrt{\frac{s}{d}}a_1(s)e^{-\sqrt{s/d}\,x} + \sqrt{\frac{s}{d}}a_2(s)e^{\sqrt{s/d}\,x}. \tag{20}$$

Letting $x = 0$ in (20) and using (12), one has

$$-\sqrt{\frac{s}{d}}e^{-\sqrt{s/d}\,h}a_1(s) + \sqrt{\frac{s}{d}}e^{\sqrt{s/d}\,h}a_2(s) = 0. \tag{21}$$

From (19) and (21), $a_1(s)$ and $a_2(s)$ can be solved. Then one can obtain the following analytical solution to (17):

$$C_1(x,s) = \frac{KC_0\varepsilon_0 e^{\sqrt{\frac{s}{d}}h}}{e^{\sqrt{\frac{s}{d}}h} + e^{-\sqrt{\frac{s}{d}}h}}e^{-\sqrt{\frac{s}{d}}x} + \frac{KC_0\varepsilon_0 e^{-\sqrt{\frac{s}{d}}h}}{e^{\sqrt{\frac{s}{d}}h} + e^{-\sqrt{\frac{s}{d}}h}}e^{\sqrt{\frac{s}{d}}x}. \tag{22}$$

Furthermore one can obtain the expression of $D(x,s)$ from (13) as follows

$$D = -FKC_0\varepsilon_0\sqrt{\frac{d}{s}}\left[\frac{e^{\sqrt{\frac{s}{d}}(x-h)}}{e^{\sqrt{\frac{s}{d}}h} + e^{-\sqrt{\frac{s}{d}}h}} - \frac{e^{-\sqrt{\frac{s}{d}}(x-h)}}{e^{\sqrt{\frac{s}{d}}h} + e^{-\sqrt{\frac{s}{d}}h}} + \tanh(h\sqrt{\frac{s}{d}})\right] - FC_0x. \tag{23}$$

Substitute (23) into (3), one has

$$\phi(x,s) - \phi(0,s) = \frac{dFKC_0\varepsilon_0}{s\kappa_e}\left[\frac{e^{\sqrt{\frac{s}{d}}(x-h)} + e^{-\sqrt{\frac{s}{d}}(x-h)}}{e^{\sqrt{\frac{s}{d}}h} + e^{-\sqrt{\frac{s}{d}}h}} + x\sqrt{\frac{s}{d}}\tanh(h\sqrt{\frac{s}{d}}) - 1\right] + \frac{FC_0}{2\kappa_e}x^2. \tag{24}$$

Thus the potential difference across one PPy layer is

$$\begin{aligned}\Delta V_1 &= \phi(h,s) - \phi(0,s) \\ &= \frac{dFKC_0\varepsilon_0}{s\kappa_e}\left[\frac{2}{e^{\sqrt{\frac{s}{d}}h} + e^{-\sqrt{\frac{s}{d}}h}} + h\sqrt{\frac{s}{d}}\tanh(h\sqrt{\frac{s}{d}}) - 1\right] + \frac{FC_0}{2\kappa_e}h^2.\end{aligned} \tag{25}$$

Due to the symmetry of the trilayer structure, the potential across the other PPy layer is

$$\Delta V_2 = -\frac{dFKC_0\varepsilon_0}{s\kappa_e}\left[\frac{2}{e^{\sqrt{\frac{s}{d}}h}+e^{-\sqrt{\frac{s}{d}}h}}+h\sqrt{\frac{s}{d}}\tanh(h\sqrt{\frac{s}{d}})-1\right]+\frac{FC_0}{2\kappa_e}h^2. \tag{26}$$

Therefore, an analytical model for the total open-circuit sensing voltage (15) is:

$$\begin{aligned} V &= \Delta V_1 - \Delta V_2 \\ &= \frac{2dFKC_0\varepsilon_0}{s\kappa_e}\left[\frac{2}{e^{\sqrt{\frac{s}{d}}h}+e^{-\sqrt{\frac{s}{d}}h}}+h\sqrt{\frac{s}{d}}\tanh(h\sqrt{\frac{s}{d}})-1\right]. \end{aligned} \tag{27}$$

From (27), one can obtain the transfer function relating the sensing voltage $V(s)$ to the applied deformation $\varepsilon_0(s)$ (strain at the PPy/PVDF interface):

$$\frac{V(s)}{\varepsilon_0(s)} = \frac{2dFKC_0}{s\kappa_e}\left[\frac{2}{e^{\sqrt{\frac{s}{d}}h}+e^{-\sqrt{\frac{s}{d}}h}}+h\sqrt{\frac{s}{d}}\tanh(h\sqrt{\frac{s}{d}})-1\right]. \tag{28}$$

We have compared the numerical solution of the full model with the analytical model derived above. In the computation, C_0 was taken to be 0.05 M. A sequence of sinusoidal inputs $\varepsilon_0(t)$, up to 100 Hz, was used. For each input, the numerical solution of $V(t)$ was computed, and the gain and phase shift at that frequency were evaluated. Fig. 2 compares the Bode plots obtained through numerical computation with those of the analytical model (28). As one can see, overall the discrepancy is not significant; in particular, as the frequency gets high, the discrepancy vanishes.

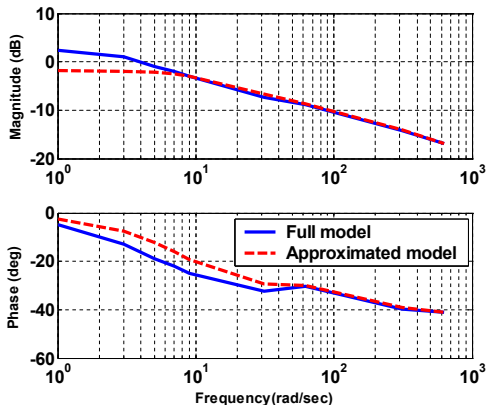

Figure 2. Comparison between the numerical solution of the full model (15) and the analytical solution of the simplified model (28) when C_0 is 0.05 M.

3. EXPERIMENTS AND DISCUSSIONS

3.1. Materials

The trilayer conjugated polymer is fabricated by the Intelligent Polymer Research Institute at the University of Wollongong. The PVDF layer is 110 μm thick and the PPy layer is 30 μm. The electrolyte used is 0.05 M tetrabutylammonium hexafluorophosphate ($TBA^+PF_6^-$) in the solvent propylene carbonate (PC). All the samples are soaked in the electrolyte for over 6 hours before experiments. Experiments were conducted at temperatures between 22 and 24 °C.

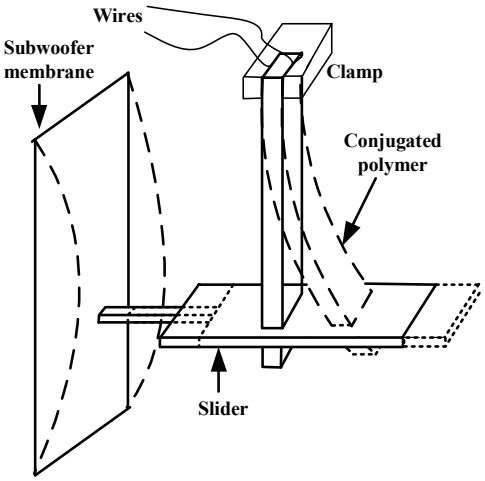

Figure 3. Schematic of the experimental setup for applying mechanical stimuli.

3.2. Experimental setup

A trilayer conjugated polymer beam is clamped on one end, where the contact electrodes are made of copper tape coated with silver. The tip of the beam is inserted into the slot of a slider, which is actuated through the membrane of a subwoofer. The apparatus can generate well-controlled sinusoidal displacements up to hundreds of Hz. This setup is illustrated in Fig. 3. The sensing voltage across the conjugated polymer beam is firstly amplified with low-noise amplifier (OPA111) and then recorded with DS1104 R&D Controller Board (dSPACE Inc).

The tip displacement of the beam is measured by a laser distance sensor (OADM 20I6441/S14F, Baumer Electric) with resolution of 5 μm. The curvature of the beam κ can be obtained via the tip displacement $y = d_0 - d$ as follows:

$$\kappa = \frac{1}{r} = \frac{2y}{y^2 + l^2}, \tag{29}$$

where l is the distance between the clamped end and the position of the laser point when the beam is not bent. When $y \ll l$, (29) can be approximated by

$$\kappa \approx \frac{2y}{l^2}. \tag{30}$$

For the ease of describing the strain, the coordinate system is defined as in Fig. 5.

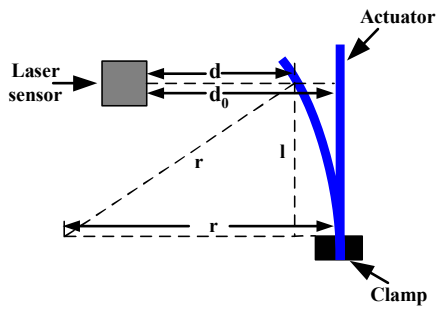

Figure 4. Geometric relationship between the beam curvature and the tip displacement.

The following equation holds for the strain and curvature

$$\varepsilon(x) = \kappa \cdot x. \tag{31}$$

Figure 5. Illustration of the trilayer structure.

Combine (30) and (31), one obtains the stress at the boundary of PPy layer and PVDF layer by letting $x = h_{PVDF}$

$$\varepsilon_0 = \frac{2h_{PVDF}}{l^2} y. \tag{32}$$

Now taking the applied tip displacement y as the input, from (28), one can obtain the transfer function for the sensing dynamics:

$$\frac{V(s)}{Y(s)} = \frac{4dFKC_0 h_{PVDF}}{sl^2\kappa_e}\left[\frac{2}{e^{\sqrt{\frac{s}{d}}h}+e^{-\sqrt{\frac{s}{d}}h}} + h\sqrt{\frac{s}{d}}\tanh(h\sqrt{\frac{s}{d}}) - 1\right]. \tag{33}$$

Sinusoidal displacement signals are applied to different samples with frequencies from 3 to 250 rad/sec. Two sets of experiments are conducted. In the first set, responses of samples with different widths but same length are compared. In the second set, responses of samples with different lengths but same width are compared. The Bode plots are utilized to compare the experimental data and model predictions in the frequency domain.

3.3. Results and discussions

Fig. 6 and Fig. 7 show the experimental characterization of the dynamic sensing behavior of the conjugated polymer samples. Predictions from the model (33) are also shown in the figures for comparison purposes. The parameters used for the model are listed in Table 1. It can be seen that the predictions from the analytical model in general fit the experimental data. In particular, the magnitude plots show good fitting with the experimental data and predict the decaying trend as the frequency becomes higher. Although there is some discrepancy in the phase plots, the general trend of the experimental data is predicted by the model.

The model (33) predicts that the sensing voltage is independent of the sample width. This is supported by the experimental data in Fig. 6, where one can see that the sensing behaviors of three samples, with different widths, are close to each other. The model also predicts that the sample length will influence the magnitude but not the phase of the transfer function, which is again verified by the experiments (Fig. 7).

Table 1. Parameter values used for the model (33).

Parameter	Value
F	9.65×10^4 C/mol
K	0.072
h	30 μm
h_{PVDF}	55 μm
d	1×10^{-8} m^2/s
κ_e	5.31×10^{-10} C^{2}N^{-1}m^{-2}
C_0	0.1 M

4. CONCLUSIONS

In this paper a model was proposed to explain the sensing mechanism of conjugated polymers. The model accounts for the ion transport dynamics within the polymer, including both ion diffusion and electric field-induced migration. A key assumption of the model is that the applied deformation prescribes the ion concentration at the polymer/electrolyte interface. The model was further simplified by dropping the migration term. In that case, an analytical solution was

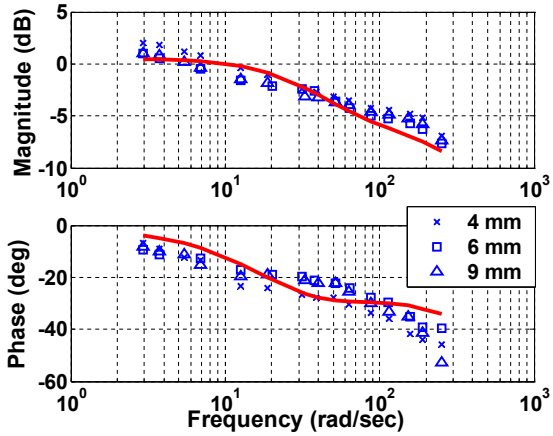

Figure 6. Dynamic response of conjugated polymer sensors: Experimental measurement (marks) versus model prediction (line). Three samples with different widths (fixed length: 30 mm).

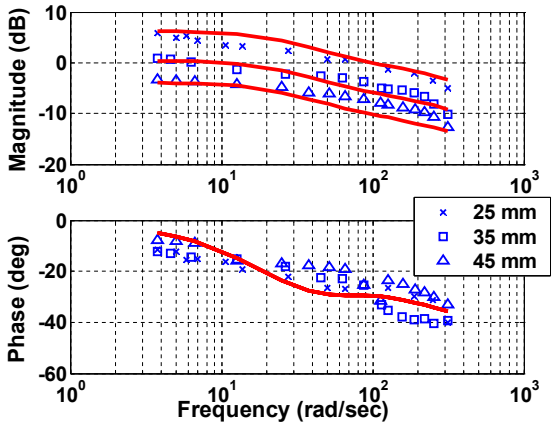

Figure 7. Dynamic response of conjugated polymer sensors: Experimental measurement (marks) versus model prediction (line). Three samples with different lengths (fixed width: 5 mm).

obtained in the Laplace domain, leading to an (infinite-dimensional) transfer function model for the sensing dynamics. Experimental results were also reported to support the modeling effort.

Despite the general success of the proposed model, there is still appreciable discrepancy between the model prediction and experimental measurement on some fine details of the sensing behavior. Clarification of the discrepancy and refinement of the model will be the focus of future work.

Acknowledgement

This research was supported in part by an NSF CAREER grant (ECS 0547131) and MSU IRGP (05-IRGP-418). Useful discussions with Mr. Hua Deng from Mechanical Engineering of Michigan State University are gratefully acknowledged.

REFERENCES

1. S. Nemat-Nasser and J. Li, "Electromechanical response of ionic polymer-metal composites," *Journal of Applied Physics* **87**, pp. 3321–3331, 2000.
2. K. Farinholt and D. J. Leo, "Modeling of electromechanical charge sensing in ionic polymer transducers," *Mechanics of Materials* **36**, pp. 421–433, 2004.
3. Y. Osada and J. P. Gong, "Soft and wet materials : Polymer gels," *Advanced Materials* **10**, pp. 827–837, 1998.

4. Z. Chen and X. Tan, "A dynamic model for ionic polymer-metal composite sensors," *Smart Materials and Structures* **16**, pp. 1477–1488, 2007.
5. W. Takashima, T. Uesugi, M. Fukui, M. Kaneko, and K. Kaneto, "Mechanochemoelectrical effect of polyaniline film," *Synthetic Metals* **85**, pp. 1395–1396, 1997.
6. J. D. W. Madden, *Conducting Polymer Actuators*. Phd thesis, MIT, 2000.
7. P. G. A. Madden, *Development and Modeling of Conducting Polymer Actuators and the Fabrication of a Conducting Polymer Based Feedback Loop*. Phd thesis, MIT, 2003.
8. Y. Fang, X. Tan, and G. Alici, "Robust adaptive control of conjugated polymer actuators," *IEEE Transactions on Control Systems Technology* , 2007. to appear.
9. Y. Fang, X. Tan, Y. Shen, N. Xi, and G. Alici, "A scalable model for trilayer conjugated polymer actuators and its experimental validation," *Materials Science and Engineering C: Biomimetic and Supramolecular Systems* , 2007. to appear.
10. G. Alici, B. Mui, and C. Cook, "Characterisation and bending modeling of conducting polymer actuators for use in micro/nano manipulation," in *Proceedings of the IEEE International Conference on Robotics and Biomimetics*, pp. 560–565, 2005.
11. Y. Wu, G. Alici, J. D. Madden, G. M. Spinks, and G. G. Wallace, "Soft mechanical sensors through reverse actuation in polypyrrole," *Advanced Functional Materialss* **17**, pp. 3216–3222, 2007.
12. W. Takashima, K.Hayasi, and K. Kaneto, "Force detection with Donnan equilibrium in polypyrrole film," *Electrochemistry Communications* **9**, pp. 2056–2061, 2007.
13. N. Lakshminarayanaiah, *Transport Phenomena in Membranes*, Academic Press, 1969.